

Research Article

Error Handling Method for Improving BDS Monitoring Accuracy of Bridge Deformation

Longsheng Bao, Tianyang Tao , and Ling Yu 

School of Transportation Engineering, Shenyang Jianzhu University, Shenyang 110168, China

Correspondence should be addressed to Tianyang Tao; 243448192@qq.com and Ling Yu; 1271840645@qq.com

Received 29 July 2021; Revised 28 December 2021; Accepted 7 February 2022; Published 8 March 2022

Academic Editor: Zhen Xu

Copyright © 2022 Longsheng Bao et al. This is an open access article distributed under the Creative Commons Attribution License, which permits unrestricted use, distribution, and reproduction in any medium, provided the original work is properly cited.

The existing high-tech bridge deformation monitoring technologies mostly use the GPS system. To eliminate the dependence on this system, China has independently developed and built the Beidou satellite navigation system. In this study, an improved algorithm for differently modulated signals is proposed to increase the accuracy of satellite monitoring and minimise the intercode interference into the output signals of the Beidou bridge deformation monitoring system. It includes a modified recurrent least square constant modulus algorithm (RLS-CMA) developed using MATLAB software. The numbers of iterations for four modulated signals are determined through various blind equalisation and intersymbol interference (ISI) algorithms as well as by performing error vector magnitude comparison simulations without equalisation, with CMA equalisation, and with enhanced RLS-CMA equalisation. At high signal-to-noise ratios, the correction speed and anti-intercode interference capability of the improved RLS-CMA are greater than those of the CMA. Moreover, the lower the error vector amplitude, the higher is the accuracy of received constellations. The error vector amplitude achieved by the RLS-CMA equalisation algorithm is lower than those of the CMA equalisation and nonequalisation algorithms, while its accuracy is increased by 17%. Hence, the improved RLS-CMA can eliminate ISI, increase the accuracy of satellite monitoring, and satisfy the requirements of theoretical analysis, calculation accuracy, and engineering error.

1. Introduction

During satellite positioning and monitoring, the most important factor affecting the communication quality is the signal intercode interference into the transmission process, which can be minimised by applying equalisation technology. In 1965, Lucky proposed a 'forced zero adaptive equaliser' according to a minimax criterion, which was used to automatically adjust the tap weighting coefficient of the horizontal equaliser [1]. In 1966, he extended this algorithm to the tracking mode, which made a significant contribution to the development of an adaptive equaliser [2]. In 1965, Ditoro independently applied adaptive equalisers to counter the effects of intersymbol interference (ISI) on the data transmission over high-frequency links [3, 4]. In 1967, Austin proposed a decision-feedback equaliser [5]. In 1969, Gersho et al. independently redefined the adaptive equaliser problem using a minimum mean square deviation criterion

[6]. In 1970, Brady proposed a fractional interval adaptive equaliser [7, 8]. In 1974, Godaard applied Kalman's filter theory to derive an efficient and fast Kalman algorithm for adjusting the tap weighting coefficient of a transverse equalisation filter [9]. In 1978, Falconer and Ljung developed another fast Kalman algorithm [10]. In 1978, Falconer and Ljung modified the fast Kalman algorithm to reduce its computational complexity to a level comparable to that of simple least mean squares (LMS) algorithms [11, 12]. Satorius and Alexander (1979) and Satorius and Pack (1981) demonstrated the applicability of this algorithm for the dispersion channel lattice-type adaptive equalisers [13].

Because the signal in a receiving channel varies due to interferences, an adaptive equaliser is frequently employed [14]. It can automatically track and cancel the interference information according to the change in the channel signal [15]. Currently, this technology represents one of the most critical methods utilised in signal-processing systems.

Because of its importance in the signal processing field, this work describes various optimised modulation signal methods and proposes a novel recurrent least square constant modulus algorithm (RLS-CMA) based on blind equalisation.

2. Research Background

By considering a long-span cable-stayed bridge in Zhejiang as an application case, this study verifies that the starting and ending piles of cable-stayed bridges are of the K313 + 526 – K317 + 515 types. The span of the navigable hole main bridge containing double towers and double cable-plane composite beams is (50 + 110 + 380 + 110 + 50) m. The structure under the bridge uses the wall pier and bored pile; the main cable tower on the bridge deck is an 'A'-type tower body; and the lower cap structure is a dumbbell-type structure. In addition, the integral auxiliary and transition piers include integral caps. The research background in this section is provided for Section 5 which contains specific research data.

3. Model Design and Production

3.1. Blind Equalisation System Model. An equivalent model of the blind equalisation system is shown in Figure 1 [16].

Here, $a(k)$ represents the original signal sequence of satellite signals. $h(h)$ refers to the impact response in the transmission channel, and $n(k)$ denotes the additive white Gaussian noise. The satellite signals received by the receiver are used as the equaliser input signals, where $w(k)$ represents the weight vector of the equaliser. $y(k)$ refers to the equalised output signal, and $a'(k)$ represents the decision output signal obtained for the $a(k)$ data evaluation [17]. Therefore, the relationship between the relevant parameter variables and the received signals in the schematic diagram of the blind balancing system above is expressed as follows:

$$x(k) = h(k) * a(k) + n(k). \quad (1)$$

Deconvolution processing is conducted to recover the original signal $a(k)$ from the distorted signal $x(k)$ [18]. If the sum of $x(k)$ and $a(k)$ is known, then deconvolution is easier to perform. However, when only $x(k)$ is known and the other parameters are unknown, this problem becomes complex and is called a blind deconvolution problem.

The blind equaliser with higher efficiency mainly uses a finite-length tapped transverse filter, whose signal input sequence is $X(k) = [X(k), X(k.1)... Y(K.L + 1)]^T$, and the weighted vector or tapped coefficient vector is $W(k) = [W0(k), W0(k)..., W.L1(k)]^T$ [19]. The relationship between parameters of the output signal of the transverse filter is expressed as follows:

$$a'(k) = \sum_{i=0}^{L-1} w_i(k)x(k-i) = X^T(k)W(k) = W^T(k)X(k). \quad (2)$$

Here, L is the equaliser length.

3.2. Blind Equalisation Algorithm. The blind equalisation technology is a special signal processing technology that uses the basic signal statistical characteristics of the channel output and input to equalise the signal emission characteristics in the channel. For this reason, it is called blind equalisation [20]. At the same time, the algorithm exhibits high convergence speed and small mean square error; therefore, its practical application value is relatively high [21].

The basic steps of the CMA are as follows.

Step 1. Initialise

$$w(0) = [0 \dots 000 \dots 0], R_p = \frac{E\{|s(n)|^4\}}{E\{|s(n)|^2\}} \quad (3)$$

Step 2. Update when $n = n + 1$:

$$y(n) = x^T(n)w(n), \quad w(n+1) = w(n) + \mu y(n) [R_2 - |Y(n)|^2] x(n). \quad (4)$$

The expression presented above indicates that the updating process of the tapping coefficient in the CMA is closely related to the statistical characteristics of received signals. However, no relevant operational relationship between the updating process of the tapping coefficient and the estimated error signal $e(n) = d(n) - y(n)$ has been established.

For example, a quadrature phase shift keying (QPSK) modulation signal can be used as the transmitted signal. In this case, the excitation channel will be interfered by the additive white Gaussian noise with a signal-to-noise ratio (SNR) of 30 dB. During algorithm processing, the system will try to use the CMA blind equaliser to recover the original signal (processing with MATLAB software is illustrated in Figure 2).

The pskSignal function's user-defined program is described as follows:

```
Function[s,a] = Signal(M,L,iniphase).
xx = [0:1:M.1]';
a = pskmod(xx,M,iniphase);
aa = randint(L,1,M);
s = pskmod(aa,M,iniphase);
s = s,';
```

A performance comparison of the CMA and LMS algorithm using MATLAB software is displayed in Figure 3. Their convergences curves show that the CMA produces an apparent equalisation effect and has high convergence speed. Figure 4 compares the convergence curves of both algorithms. It shows that the convergence rate of the CMA is greater while its mean square error is lower than the corresponding parameters of the LMS algorithm.

The basic parameters are set as follows:

for $jj = 1:m$.

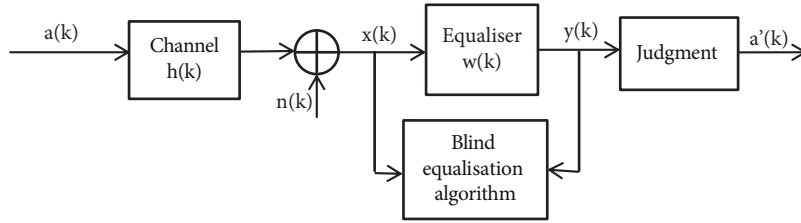


FIGURE 1: Schematic diagram of blind equalisation system.

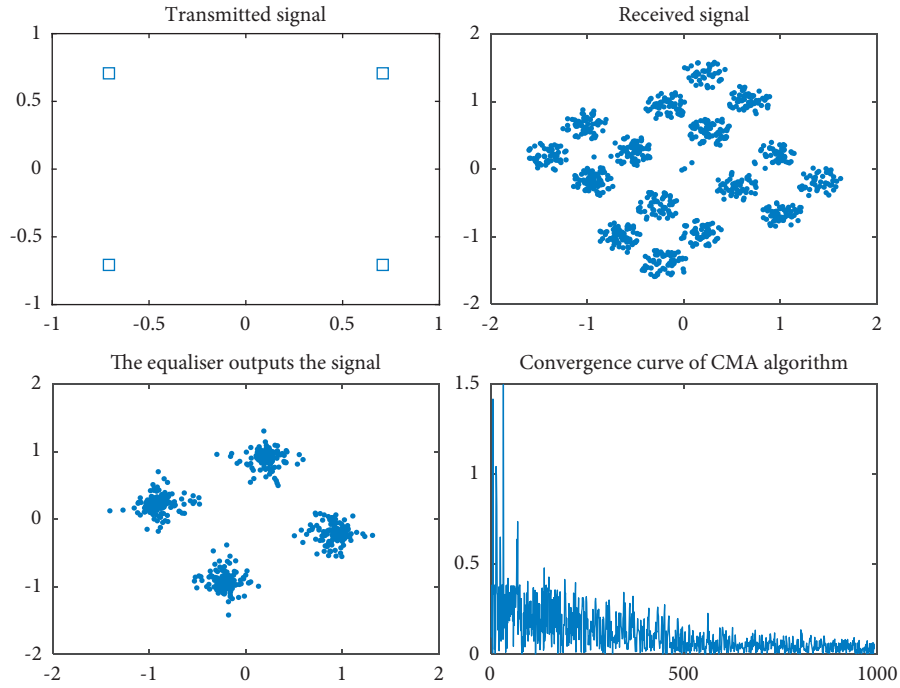


FIGURE 2: Equalisation effect of the CMA.

```

a = randi([0,M-1],1,n);
a1 = pskmod(a,M);
m1 = abs(a1)/4;
m2 = abs(a1)/2;
r1 = mean(m1);
r2 = mean(m2);
R2 = r1/r2;
%R2 = sqrt(2%);
s = filter(h,1,a1);
snr = 15;
x = awgn(s,snr,'measured');
c1 = [0 0 0 1 0 0 0];
c2 = c1;
y = zeros(n-L+1,2);
for ii = 1:n-L+1.
y = x(ii + L - 1:-1:ii);

```

```

z1(ii) = c1 * y';
z2(ii) = c2 * y';
e1 = R2 - (abs(z1(ii)))^2;
e2 = a1(ii) - z2(ii);
c1 = c1 + u1 * e1 * y * z1(ii);
c2 = c2 + u2 * e2 * y;
mse1(ii) = e1^2;
%u(i) = 0.2 * (1 - exp(-(0.3 * abs(e(i)))));
mse2(ii) = abs(e2)^2;
end;

```

3.3. *Improved RLS-CMA*. First, the least squares criterion is defined as follows:

$$W(k) = W(k-1) + u(k)e * (k). \quad (5)$$

Here, $e(k) = d(k) - W(k-1)^H X(k)$ is the prior estimate error;

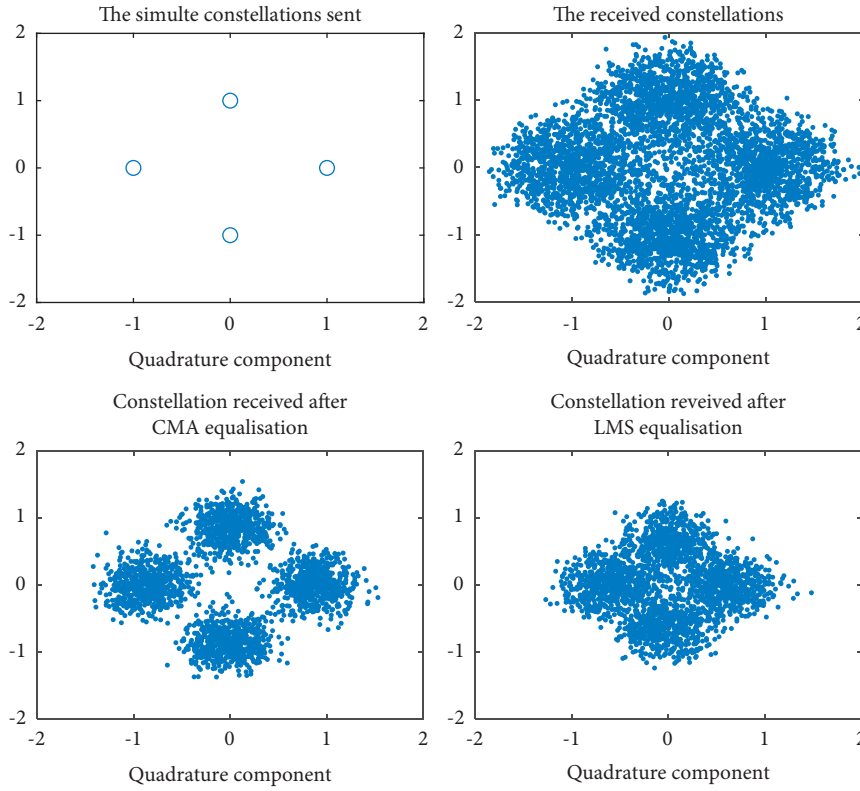


FIGURE 3: QPSK modulations equalised by the CMA and LMS algorithm for a constellation comparison.

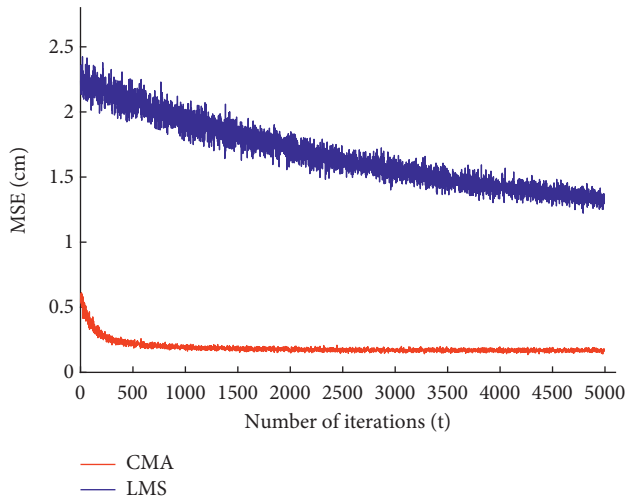


FIGURE 4: Convergence curves obtained for the CMA and LMS algorithm.

$u(k) = P(k-1)X(k)/\lambda + X(k)^H P(k-1)X(k)$ is called the gain vector; and

$$P(k) = \frac{1}{\lambda} \left[P(k-1) - \frac{P(k-1)X(k)X(k)^H P(k-1)}{\lambda + X(k)^H P(k-1) * X(k)} \right]. \quad (6)$$

$0 < \lambda < 1$ is the forgetting factor.

With respect to the normal signal, the quality of the signal captured by a normal array is mainly affected by the initial weight vector and the strength of the array signal

output. For practical applications, the robustness of the CMA should be increased. In this study, a method for generating the initial weight vector through the iteration of the RLS algorithm described by mathematical expression (5) is mainly applied.

Based on the traditional beamforming algorithm, instead of using a constant mode signal as the user signal, the weighted vector polynomial of the algorithm is applied to obtain the arrival angle of other users, which is true not only for the constant mode signal but also for other signals. Therefore, this work combines the RLS algorithm with the CMA to realise the separate acceptance of multiple signals.

In this study, binary phase shift keying (BPSK), QPSK, 8-phase shift keying (8PSK), and 16-phase shift keying (16PSK) modulations are adopted for simulations and comparative analysis. The CMA and RLS-CMA are used to achieve MPSK source equalisation on different bases. The basic MATLAB settings are described as follows:

```

i = sqrt(1);
L = 2000;
SNR = 30;
H = [0.26, 0.93, 0.26, 0.1]; %% channel coefficient.
h = h/norm(h);
Nh = length(h);
ISI_CMA = 0;
ISI_RLS_CMA = 0;
Nf = 37;

```

```

times = 25;
STR = {'BPSK modulation ', 'QPSK modulation ', '8 PSK
modulation ', '16 PSK modulation '};
M = [2 4 8 16];
Id = menu('BPSK modulation ', 'QPSK modulation ',
'8PSK modulation ', '16PSK modulation ');
for id_SNR = 1:length(SNR).

```

4. Simulation Analysis

4.1. ISI Simulation Analysis of the Improved RLS-CMA. In this study, the BPSK, QPSK, 8PSK, and 16PSK modulation modes are used as phase-shift keys, and the results of CMA and improved RLS-CMA simulations are compared and verified. Here, algorithm variables include the absolute and relative phase-shift keying points. The absolute phase shifts during simulations result in blurred images. Regarding the phase shift, the receiving device is relatively simple and can avoid phase ambiguity. Compared with the QPSK, 8PSK, and 16PSK modulations, BPSK exhibits a higher noise resistance but lower transmission efficiency [22].

The signal source is set as follows:

```

loop.
Sym_stream = randi([0 M(id).1],L,1);
modu_sig = (pskmod(sym_stream,M(id)))';
fil_sig = filter(h,1,modu_sig);
recv_sig = awgn(fil_sig,SNR(id_SNR),'measured');

```

BPSK is an important method for the signal conversion into data [23]. It uses a basic theory similar to that including sine waves and phase reversal waves to make the two ends of the phase shift keying equal to 0 and 1, respectively, and to simultaneously send and receive two information values. In the case of analogue modulation, the receiver recovers erroneously because of the reverse phase of the reference carrier. For this reason, the abovementioned approach is not very practical.

By using MATLAB software, the relationship between the number of iterations and the ISI of the BPSK modulation signal is simulated for different blind equalisation algorithms at SNR values of 15, 25, 35, and 45 dB (Figure 5). When SNR = 15 dB and the number of iterations exceeds 960, the RLS-CMA is better than the CMA in terms of ICI processing. When the number of iterations reaches approximately 1780, the RLS-CMA has the highest processing power. When SNR = 25 dB and the number of iterations is more than 200, the RLS-CMA can handle ICI better than the CMA. When the number of iterations reaches approximately 380, the RLS-CMA has the highest processing power. When SNR = 35 dB and the number of iterations exceeds 280, the RLS-CMA can handle ICI better than the CMA. When the number of iterations reaches approximately 700, the RLS-CMA has the highest processing power. When SNR = 45 dB and the number of iterations is more than 570, the RLS-CMA can handle ICI better than the CMA. When the number of iterations reaches approximately 980, the RLS-CMA has the highest processing power. Hence, it can

be concluded that, with an increase in SNR, the improved RLS-CMA is superior to the CMA in terms of the correction speed and anti-ICI capability.

QPSK is a digital modulation method [24], which can be divided into the absolute and relative phase shifts. Owing to the existence of the absolute and relative phase modes, the relative phase shift mode DQPSK is usually used in the actual algorithm to perform required operations. The sine wave in the QPSK signal has four different discrete phase states, and each of these states contains two binary symbols. The mathematical form of the signal is expressed as follows:

$$S_i(t) = A \cos(\omega_c t + \theta_i). \quad (7)$$

Therefore, between 0 and T_s , i equals 1, 2, 3, 4, where T_s is the quaternion symbol interval, and i ($i = 1, 2, 3, 4$) is the phase of the sinusoidal carrier. Thus, four different phase states can possibly exist.

It is noteworthy that the sampling clock of the analogue-to-digital converter is not extracted from the signal. If the sampling clock cannot maintain the same phase as the signal input, the statistical SNR of the sampling value at the optimal sampling time will not reach a maximum, and the bit error rate will be very high. Therefore, it is necessary to restore the clock synchronised with the input symbol rate of the circuit to correct the sampling error caused by fixed sampling.

Using MATLAB software, the relationships between the number of iterations and the ISI of the QPSK modulation signal obtained for different blind equalisation algorithms at SNR values of 15, 25, 35, and 45 dB are shown in Figure 6. When SNR = 15 dB and the number of iterations exceeds 180, the RLS-CMA can handle ICI better than the CMA. When the number of iterations reaches approximately 420, the RLS-CMA has the highest processing power. When SNR = 25 dB and the number of iterations is more than 10, the RLS-CMA is better than the CMA in terms of ICI processing. When the number of iterations is approximately 390, the RLS-CMA has the highest processing power. When SNR = 35 dB and the number of iterations exceeds 30, the RLS-CMA is better than the CMA in terms of ICI processing. When the number of iterations reaches approximately 400, the RLS-CMA has the highest processing power. When SNR = 45 dB and the number of iterations is more than 25, the RLS-CMA is superior to the CMA in terms of ICI processing. When the number of iterations reaches approximately 630, the RLS-CMA has the highest processing power. Hence, it has been concluded that, with an increase in SNR, the correction speed of the RLS-CMA and its anti-ICI capability are higher than those of the CMA.

8PSK is a phase modulation algorithm [25]. The demodulation block diagram of the 8PSK signal receiver is shown in Figure 7. By using MATLAB software, relationships between the number of iterations and ISI are established for different blind equalisation algorithms of the 8PSK modulation signal at SNR values of 15, 25, 35, and 45 dB (Figure 8). When SNR = 15 dB and the number of iterations is more than 170, the RLS-CMA is superior to the CMA in terms of ICI processing. When the number of iterations reaches approximately 290, the RLS-CMA has the highest

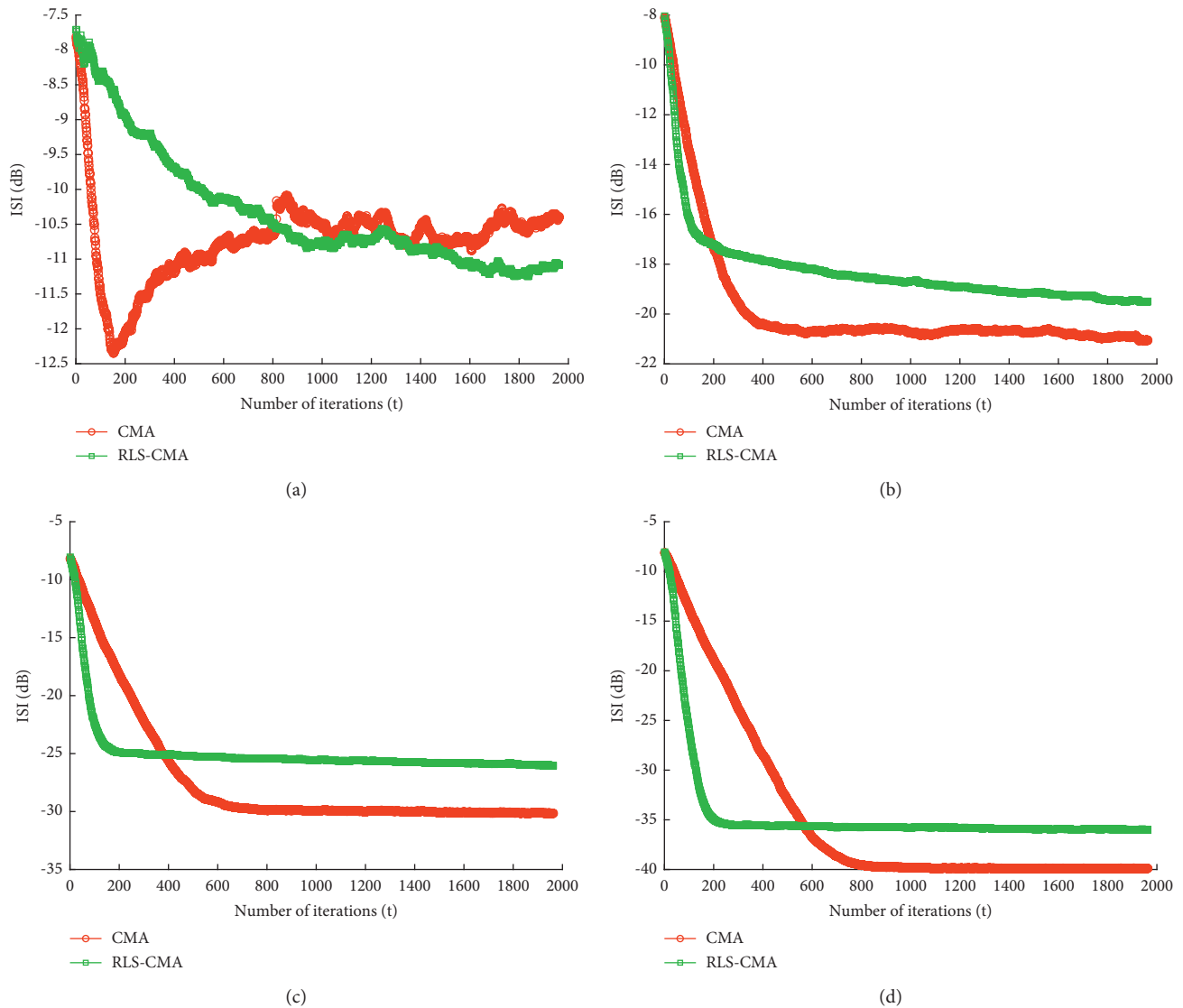


FIGURE 5: Relationships between the number of iterations and the ISI of the BPSK-modulated signal obtained for different blind equalisation algorithms. (a) SNR = 15 dB. (b) SNR = 25 dB. (c) SNR = 35 dB. (d) SNR = 45 dB.

processing power. When SNR = 25 dB and the number of iterations exceeds 80, the RLS-CMA can handle ICI better than the CMA. When the number of iterations reaches approximately 400, the RLS-CMA has the highest processing power. When SNR = 35 dB and the number of iterations exceeds 40, the RLS-CMA is better than the CMA in terms of ICI processing. When the number of iterations reaches approximately 450, the RLS-CMA has the highest processing power. When SNR = 45 dB and the number of iterations exceeds 30, the RLS-CMA can handle ICI better than the CMA. When the number of iterations reaches approximately 430, the RLS-CMA has the highest processing power. Thus, it has been concluded that, with an increase in SNR, the correction speed of the RLS-CMA and its anti-ICI capability are greater than those of the CMA.

16PSK can use 16 different carrier stages to express the corresponding digital information [26]. Using MATLAB software, relationships between the number of iterations and

the ISI of the 16PSK modulation signal are established for different blind equalisation algorithms at SNR values of 15, 25, 35, and 45 dB (Figure 9). When SNR = 15 dB and the number of iterations exceeds 200, the RLS-CMA is better than the CMA in terms of ICI processing. When the number of iterations reaches approximately 400, the RLS-CMA has the highest processing power. When SNR = 25 dB and the number of iterations is more than 160, the RLS-CMA can handle ICI better than the CMA. When the number of iterations is approximately 420, the RLS-CMA has the highest processing power. When SNR = 35 dB and the number of iterations is more than 130, the RLS-CMA can handle ICI better than the CMA. When the number of iterations is approximately 460, the RLS-CMA has the highest processing power. When SNR = 45 dB and the number of iterations is more than 100, the RLS-CMA is superior to the CMA in terms of ICI processing. When the number of iterations is approximately 610, the RLS-CMA has the highest processing

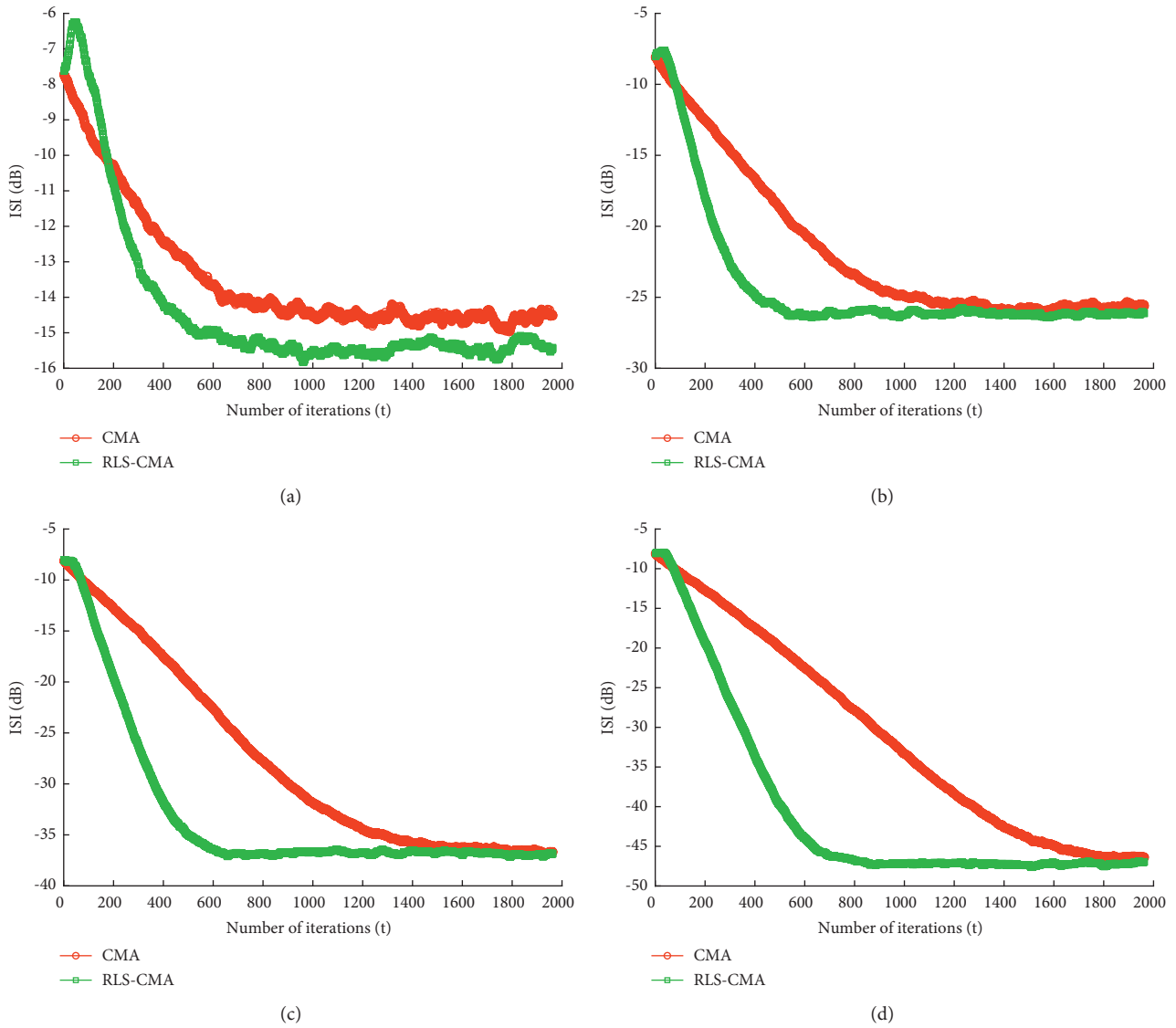


FIGURE 6: Relationships between the number of iterations and the ISI of the QPSK-modulated signal obtained for different blind equalisation algorithms at SNR = 15–45 dB: (a) SNR = 15 dB. (b) SNR = 25 dB. (c) SNR = 35 dB. (d) SNR = 45 dB.

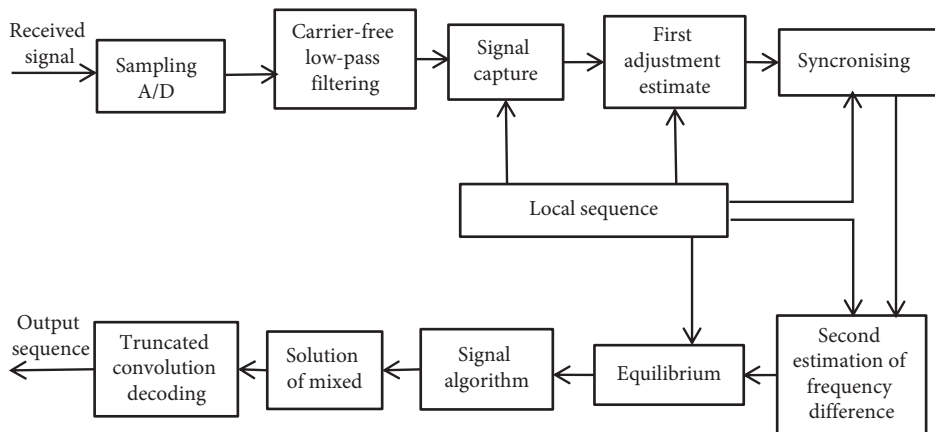


FIGURE 7: Block diagram of the 8PSK signal demodulation process.

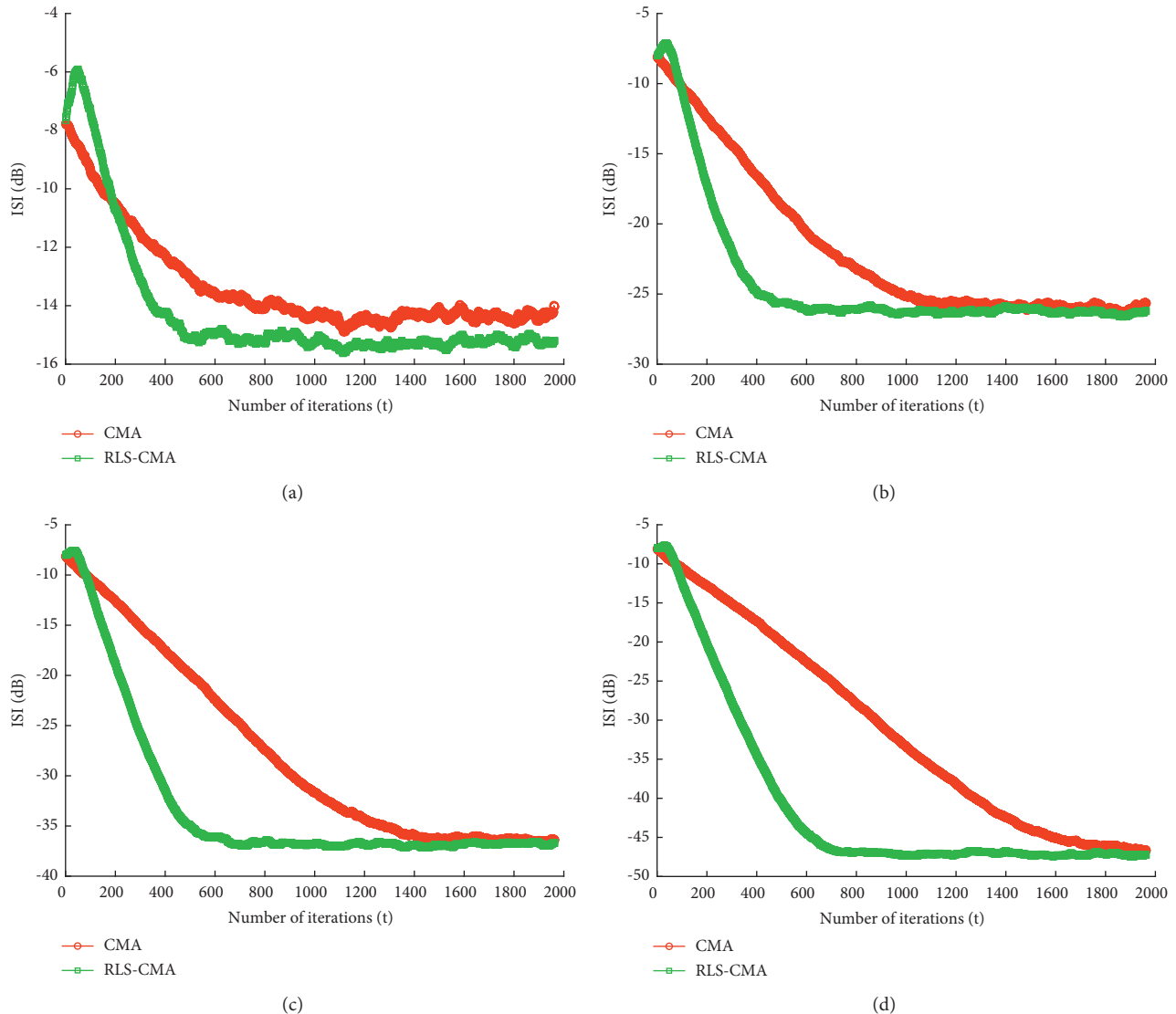


FIGURE 8: Relationships between the number of iterations and the ISI of the 8PSK-modulated signal obtained for different blind equalisation algorithms at SNR = 15–45 dB: (a) SNR = 15 dB. (b) SNR = 25 dB. (c) SNR = 35 dB. (d) SNR = 45 dB.

power. Therefore, it has been concluded that, with an increase in SNR, the RLS-CMA is significantly better than the CMA in terms of the correction speed and anti-ICI capability (Figure 9).

4.2. Error Vector Magnitude Analysis of the Improved RLS-CMA. Error vector magnitude (EVM) refers to the vector difference between the ideal transmission efficiency of a signal at a given moment and the actual transmission efficiency of the same signal. EVM can accurately measure the amplitude and phase errors of the modulated signal and thus represents an important parameter used for its quality evaluation. According to relevant research theories, the EVM error vector is closely related to the equivalent I/Q QPSK modulation mode, which is generally represented by the I/Q 'Stars' demodulation symbol.

The error vector amplitude is defined as the vector amplitude obtained by comparing the average power of the error vector signal with the average power of the ideal signal at a given moment. The smaller the EVM component in the ratio, the higher the signal quality.

The main purpose of the conducted test is to confirm whether the waveform generated by the transmitter during the signal transmission process satisfies the theoretical requirements to enhance the receiver acceptance performance. In this paper, a transmitted signal is simulated, and the data received by the receiver are processed by improved RLS-CMA and CMA, respectively.

As there are many types of modulation verification signals, the 16PSK modulation signal is selected in this study, and its detailed processing by MATLAB software is illustrated in Figures 10 and 11, which display the constellation diagrams of the BPSK modulation, QPSK modulation, 8PSK

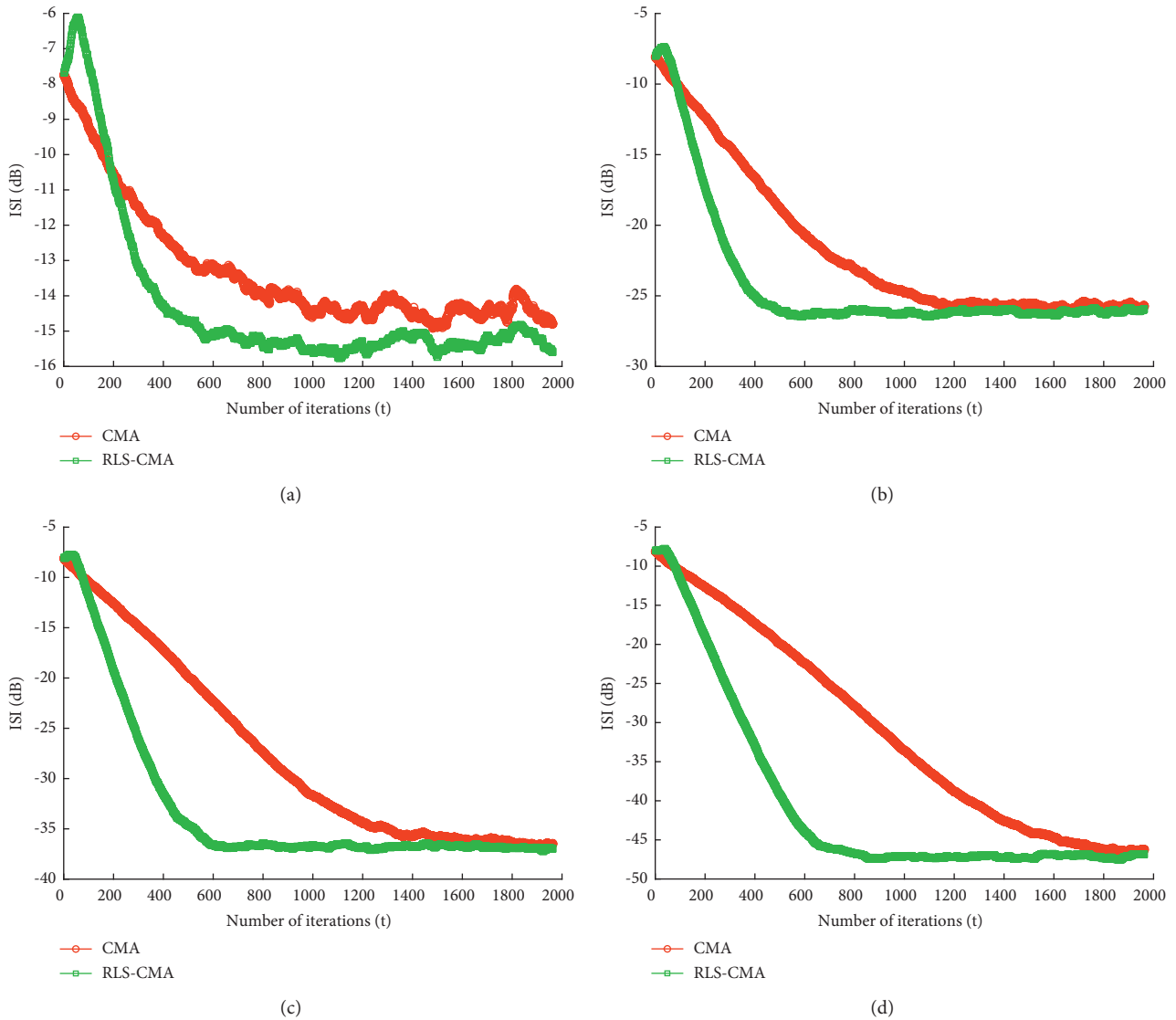


FIGURE 9: Relationships between the number of iterations and the ISI of the 16PSK-modulated signal obtained for different blind equalisation algorithms at SNR = 15–45 dB: (a) SNR = 15 dB. (b) SNR = 25 dB. (c) SNR = 35 dB. (d) SNR = 45 dB.

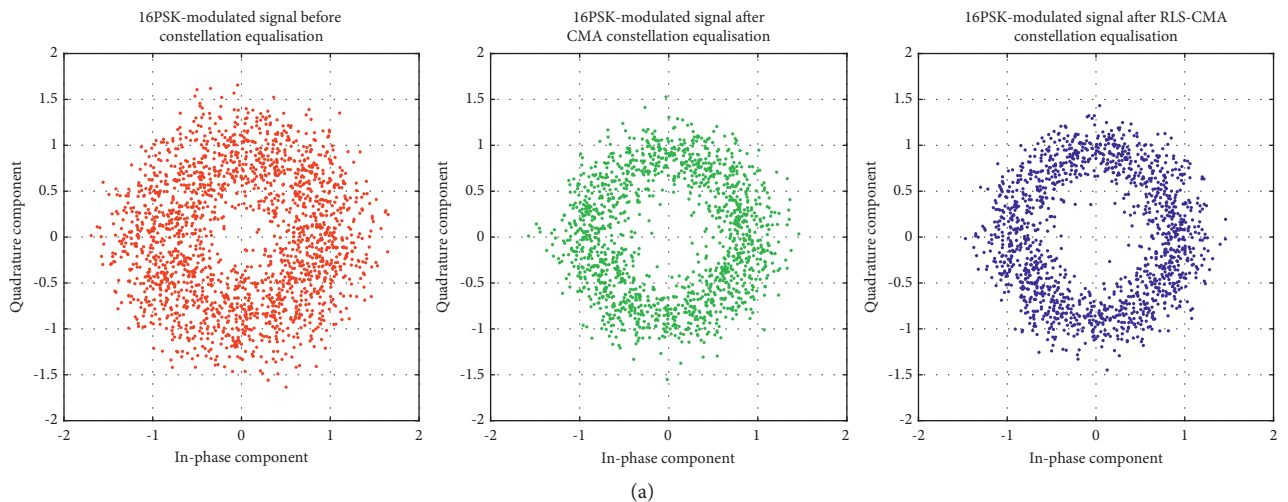


FIGURE 10: Continued.

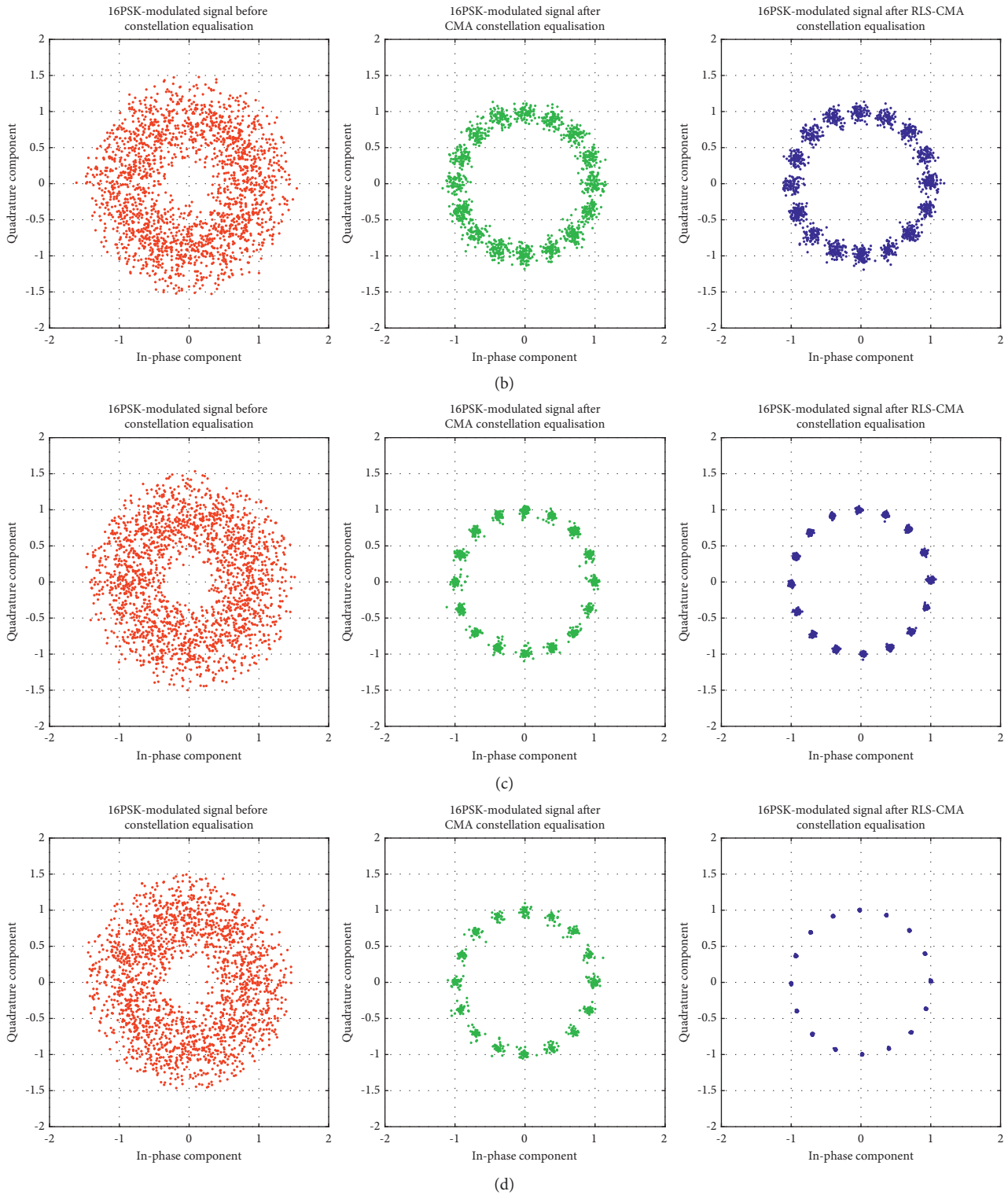


FIGURE 10: Continued.

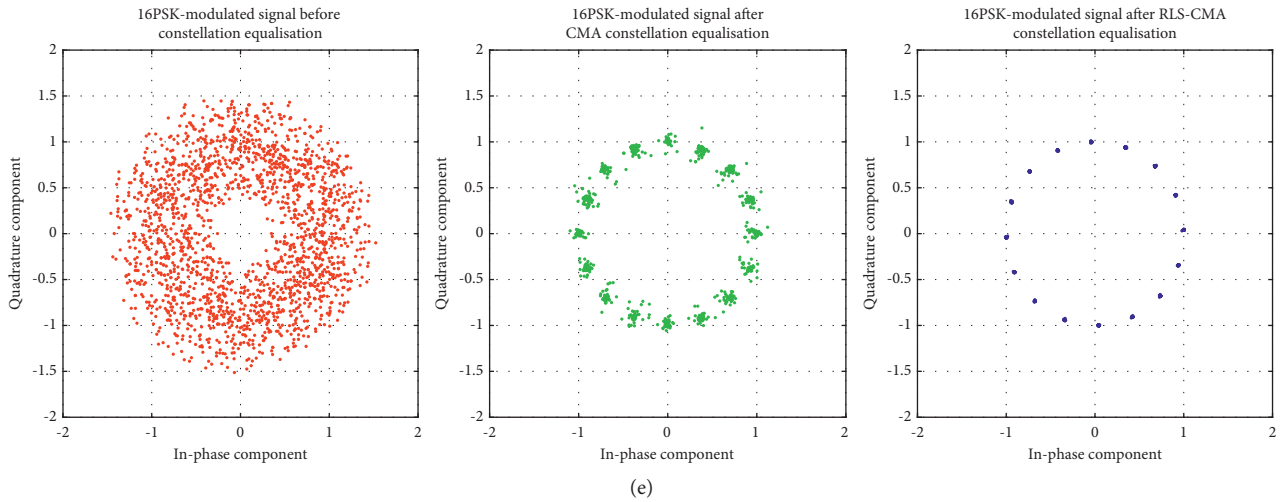


FIGURE 10: Constellations of the 16PSK-modulated signals obtained by different blind equalisation algorithms. (a) SNR = 15 dB. (b) SNR = 25 dB. (c) SNR = 35 dB. (d) SNR = 45 dB. (e) SNR = 55 dB.

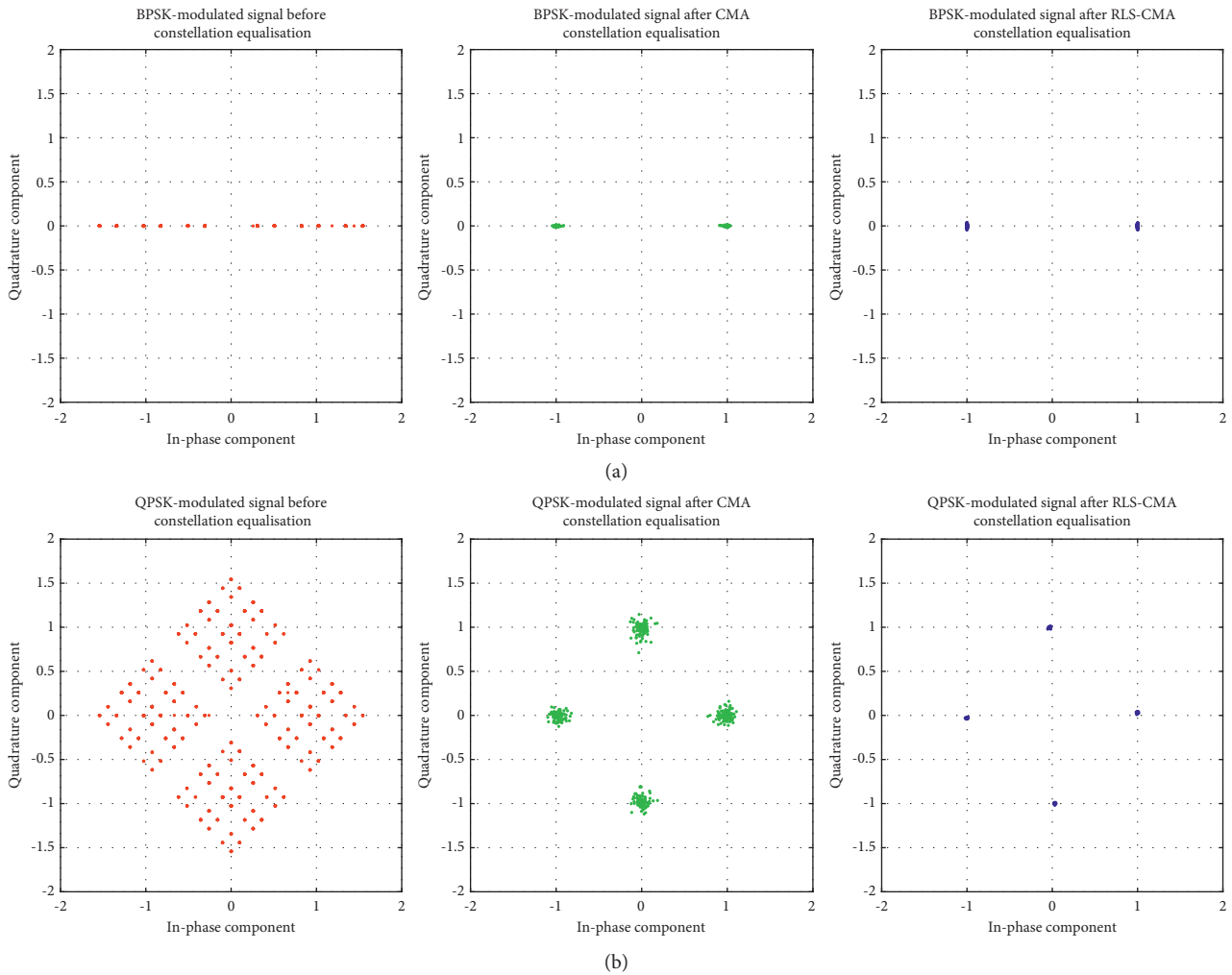


FIGURE 11: Continued.

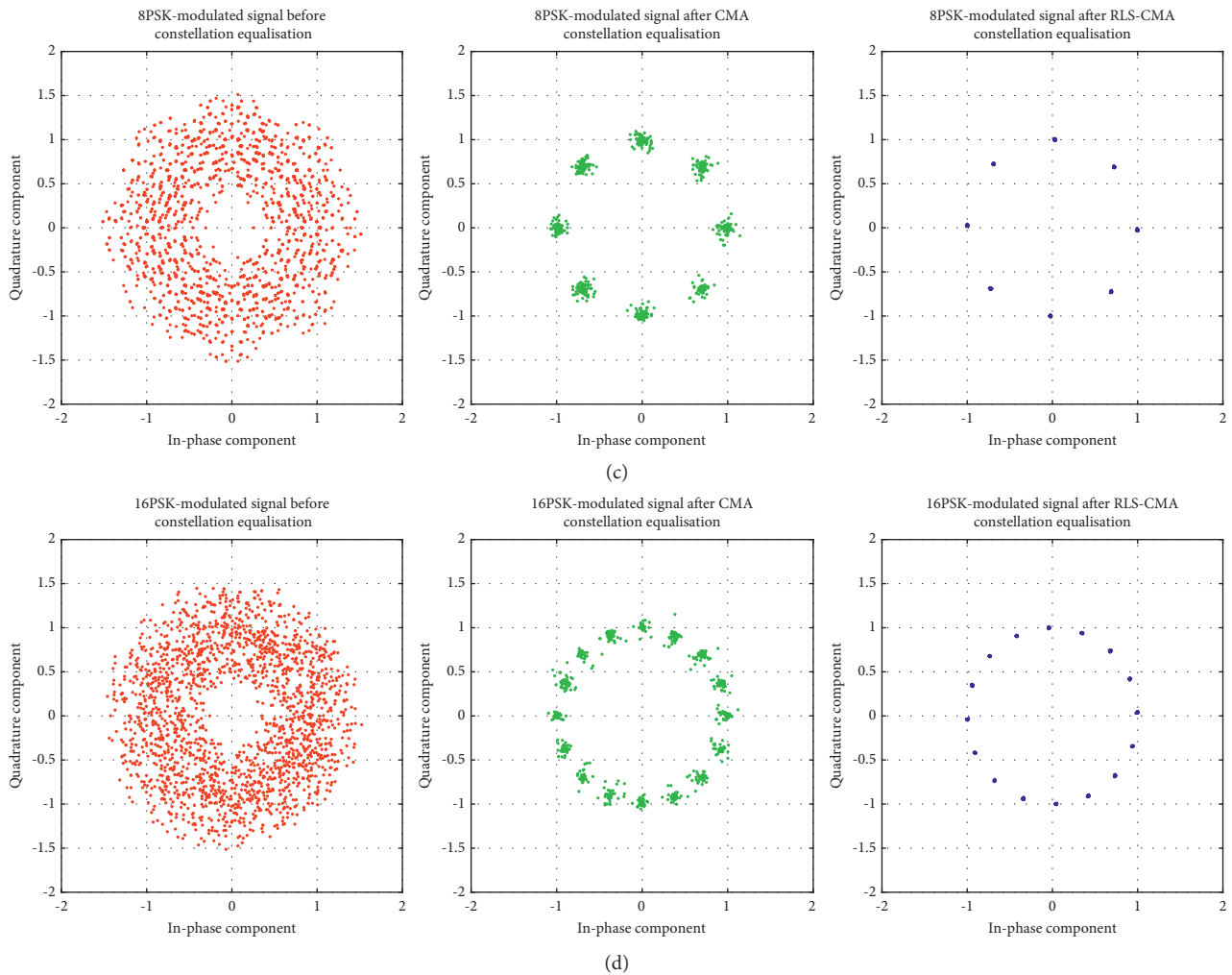


FIGURE 11: Constellations of different modulated signals obtained by the RLS-CMA blind equalisation algorithm. (a) BPSK modulation (SNR = 55 dB). (b) QPSK modulation (SNR = 55 dB). (c) 8PSK modulation (SNR = 55 dB). (d) 16 PSK modulation (SNR = 55 dB).

modulation, and 16PSK modulation processes obtained with the CMA-RLS algorithm. The results indicate that the transmitter waveform processed by the RLS-CMA is more accurate than the waveform processed by the CMA.

Finally, Figures 12–15 illustrate a comparison of the EVM simulation curves of the BPSK, QPSK, 8PSK, and 16PSK modulation signals obtained without equalisation, after CMA equalisation, and after RLS-CMA equalisation. They show that the accuracy of the RLS-CMA equalisation algorithm is higher than those of the CMA and non-equalisation algorithm, while its error vector amplitude is lower than the error vector amplitudes of the other two algorithms.

Tables 1–4 present a comparison of the error vector amplitude values of BPSK, QPSK, 8PSK, and 16PSK-modulated signals after unbalanced, CMA balanced, and RLS-CMA balanced EVM/bit. The results in Table 1 show that the error vector amplitude of the RLS-CMA equalisation algorithm is 0.0051–0.0357 bits lower than that of the CMA equalisation algorithm under different SNR values after BPSK-modulated signal equalisation. Table 2 shows that the

error vector amplitude of the RLS-CMA equalisation algorithm is 0.0162–0.0412 bits lower than that of the CMA equalisation algorithm under different SNR values after QPSK-modulated signal equalisation. Table 3 shows that the error vector amplitude of the RLS-CMA equalisation algorithm is 0.0112–0.0402 bits lower than that of the CMA equalisation algorithm under different SNR values after 8PSK-modulated signal equalisation. Table 4 shows that the error vector amplitude of the RLS-CMA equalisation algorithm is 0.0171–0.0355 bits lower than that of the CMA equalisation algorithm under different SNR values after 16PSK-modulated signal equalisation.

5. Case Validation

In this study, the proposed RLS-CMA is used for error processing. With an increase in the measurement time, the monitoring results originally affected by various errors gradually converge to the real coordinates of the monitoring points. Therefore, the longer the monitoring time, the more accurate the measurement data. Table 5 lists the standard

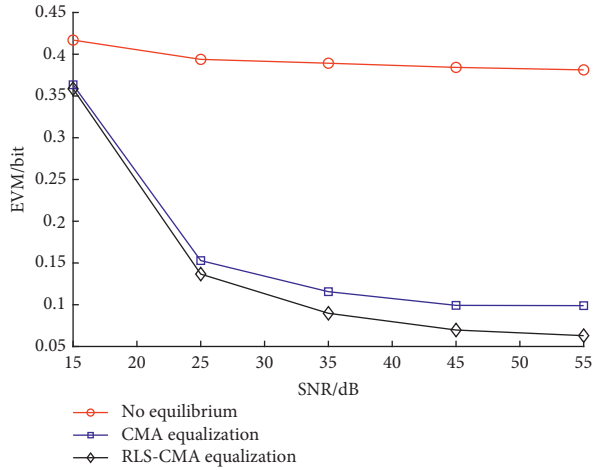


FIGURE 12: BPSK EVM curves.

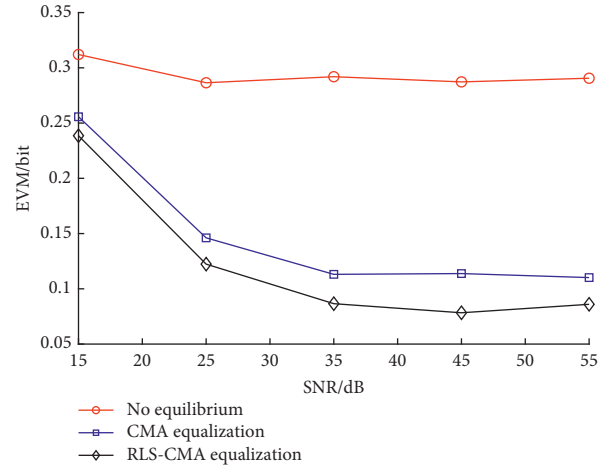


FIGURE 15: 16PSK EVM curves.

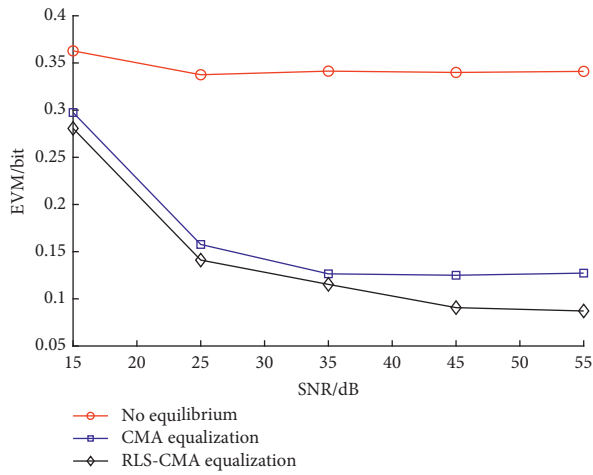


FIGURE 13: 8PSK EVM curves.

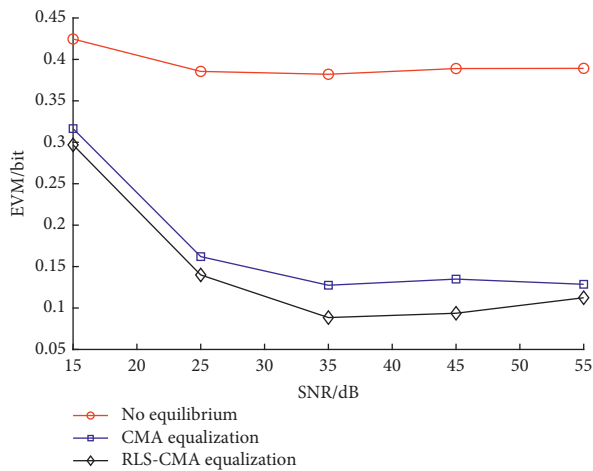


FIGURE 14: QPSK EVM curves.

TABLE 1: EVM values obtained by different blind homogeneous algorithms for the BPSK-modulated signals.

SNR/dB	15	25	35	45	55
Without a balanced EVM/bit	0.4274	0.3920	0.3954	0.3827	0.3921
CMA EVM/bit	0.3908	0.1604	0.1325	0.1011	0.0986
RLS-CMA EVM/bit	0.3799	0.1408	0.1274	0.0611	0.0629
EVM accuracy difference/bit	0.0109	0.0196	0.0051	0.0400	0.0357

TABLE 2: EVM values obtained by different blind homogeneous algorithms for the QPSK-modulated signals.

SNR/dB	15	25	35	45	55
Without a balanced EVM/bit	0.4246	0.3855	0.3821	0.3890	0.3892
CMA EVM/bit	0.3165	0.1620	0.1275	0.1349	0.1286
RLS-CMA EVM/bit	0.2969	0.1399	0.0885	0.0937	0.1124
EVM accuracy difference/bit	0.0196	0.0221	0.0390	0.0412	0.0162

TABLE 3: EVM values obtained by different blind homogeneous algorithms for the 8PSK-modulated signals.

SNR/dB	15	25	35	45	55
Without a balanced EVM/bit	0.3628	0.3375	0.3413	0.3399	0.3411
CMA EVM/bit	0.2975	0.1576	0.1265	0.1250	0.1273
RLS-CMA EVM/bit	0.2806	0.1411	0.1153	0.0907	0.0871
EVM accuracy difference/bit	0.0169	0.0165	0.0112	0.0343	0.0402

requirements for monitoring the accuracy of bridge deformation.

In Zhejiang, a large dipper of the long-span cable-stayed bridge is installed at each monitoring station. The measuring

TABLE 4: EVM values obtained by different blind homogeneous algorithms for the 16PSK-modulated signals.

SNR/dB	15	25	35	45	55
Without a balanced EVM/bit	0.3121	0.2865	0.2920	0.2873	0.2906
CMA EVM/bit	0.2557	0.1461	0.1131	0.1138	0.1102
RLS-CMA EVM/bit	0.2386	0.1223	0.0865	0.0783	0.0860
EVM accuracy difference/bit	0.0171	0.0238	0.0266	0.0355	0.0242

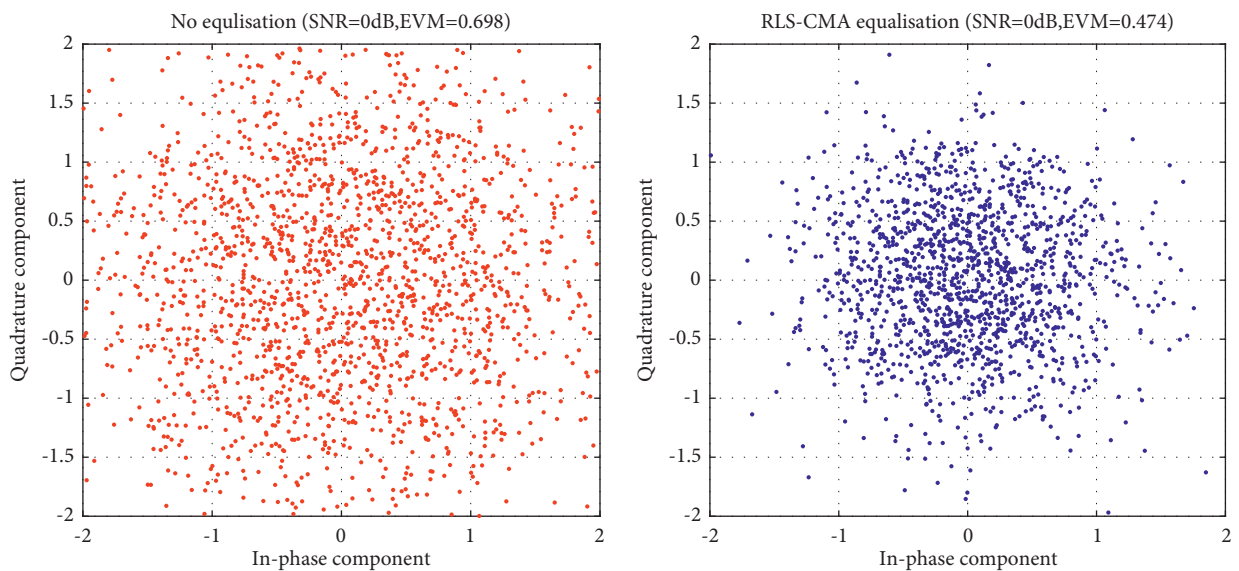
TABLE 5: System technical parameters.

Project	Content	Indicators
Positioning accuracy ¹	Real-time positioning accuracy	Horizontal level is better than 0.2 m Vertical level is better than 0.5 m
	Postprecise positioning	Horizontal level is better than 0.03 m Vertical level is better than 0.05 m
Availability ²	Navigation	95.0%
	Positioning	95.0%
Compatibility	Satellite signal	BDS B1, B2; GPS L1, L2; GLO G1, G2
	Data format	Receive raw binary data streams; RTCM3.X
	Receiver equipment	The current mainstream manufacturers of Beidou receiver
Communication mode	Real-time user	3G/4 G/Internet

Note 1: the accuracy value is a one-time medium error. Positioning accuracy refers to the accuracy of the CGCS2000 coordinate system. Note 2: the availability indicator does not consider the availability of a communication network.



FIGURE 16: Photograph of the GNSS measuring point of the bridge tower.



(a)

FIGURE 17: Continued.

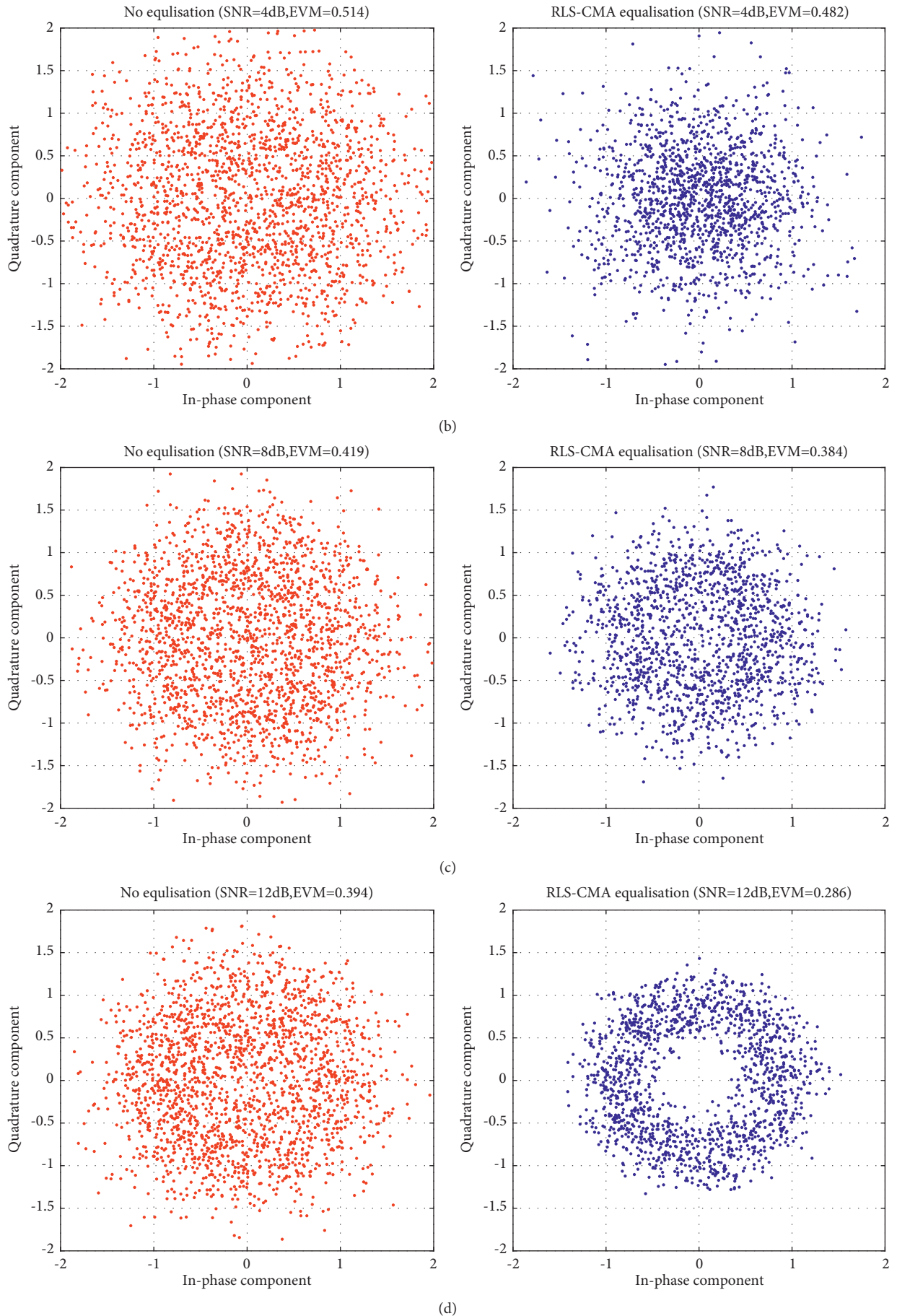


FIGURE 17: Continued.

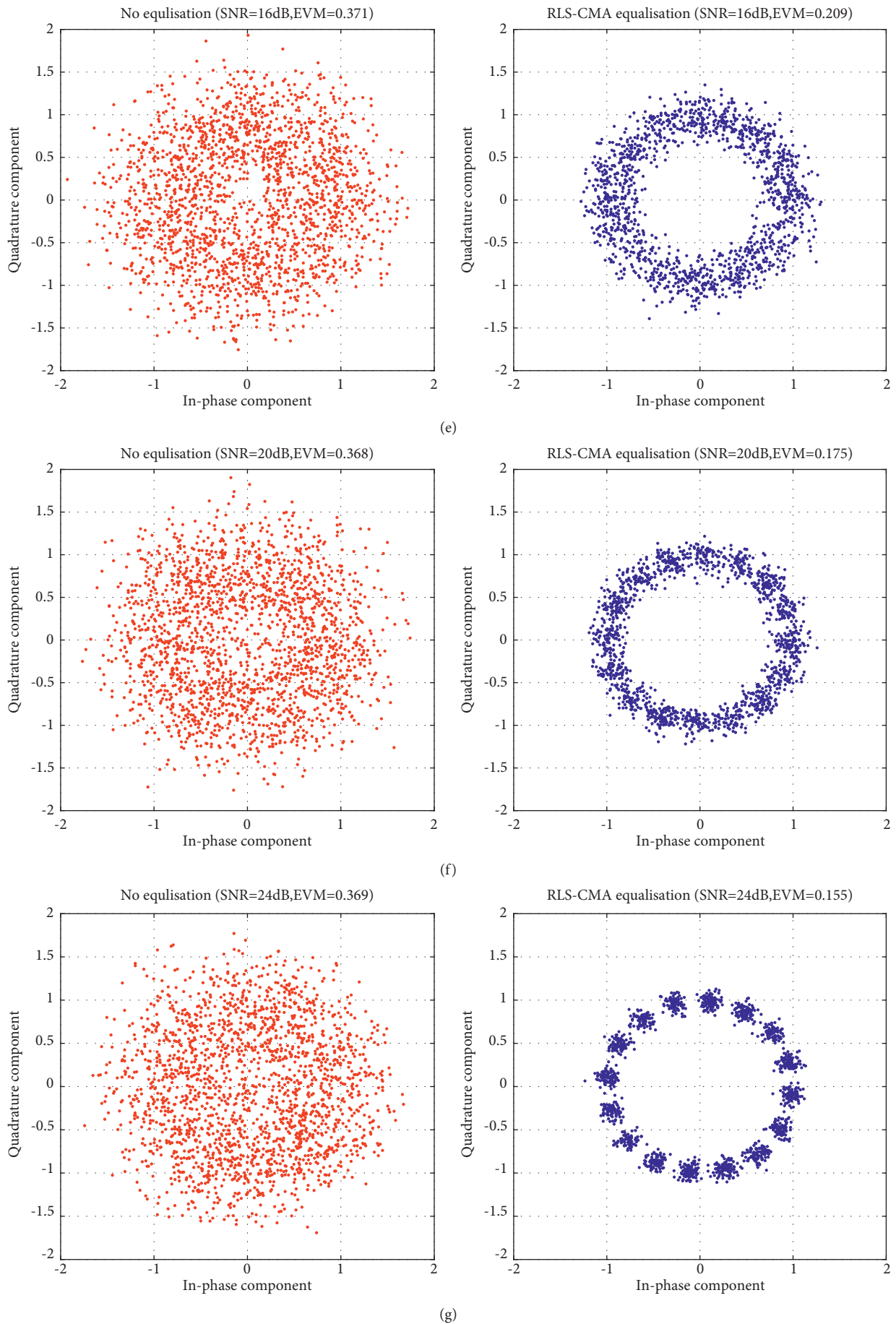


FIGURE 17: RLS-CMA equalisation of the PSK-modulated signals. (a) 16PSK SNR = 0 dB. (b) 16PSK SNR = 4 dB. (c) 16PSK SNR = 8 dB. (d) 16PSK SNR = 12 dB. (e) 16PSK SNR = 16 dB. (g) 16PSK SNR = 24 dB. (f) 16PSK SNR = 20 dB.

TABLE 6: Error vector amplitude accuracy values obtained for the 16PSK-modulated signals before and after RLS-CMA equalisation.

16PSK SNR ratio/dB	0	4	8	12	16	20	24
Without equalisation	0.682	0.510	0.430	0.387	0.379	0.366	0.361
After RLS-CMA equalisation	0.476	0.473	0.383	0.304	0.229	0.167	0.144
Precision before and after equalisation	0.206	0.037	0.047	0.083	0.150	0.199	0.217

point of the bridge tower's displacement is set at the top of the bridge tower, and the base point is set on a stable foundation within 2 km. The studied system includes one base point and three measurement points. The fixed base station with known coordinates is defined as the reference point, and the monitoring point on the bridge tower is defined as the test point. At the same time, the reference and test points are monitored to estimate the error of the monitored data. The same satellite is utilised to observe the monitoring points for a long time to ensure the accuracy of data analysis. The layout of the bridge tower GNSS measurement points is shown in Figure 16.

The original data collected by observation on February 17, 2021, is shown in Figure 17. The obtained data are modulated in the 16PSK mode, and the processing results of the improved RLS-CMA equalisation algorithm are presented in Figure 17. The results show that when the SNR reaches 24 dB, the data processed by the equalisation algorithm is converged at a higher accuracy (the actual data points are provided in Table 6).

6. Conclusions

In this study, an improved RLS-CMA based on the RLS and blind equalisation algorithms is proposed to reduce the intercode interference into the transmitted BDS monitoring signal and increase the monitoring accuracy. Unlike other methods, the improved RLS-CMA not only eliminates ICI, but also exhibits higher correction speed and anti-ICI capability than those of other algorithms. The ability of the developed algorithm to eliminate intercode interference is satisfactory, which is reflected in the results obtained in this work. After filtering the boundaries, the received signal is processed, and the improved RLS-CMA eliminates ICI more effectively, while its convergence rate is greater than that of the CMA. Hence, the proposed algorithm can considerably increase the measurement accuracy of the Beidou monitoring system and satisfy the bridge deformation monitoring requirements.

After performing a practical verification of the improved RLS-CMA, the following conclusions have been drawn:

- (1) In this work, an improved RLS-CMA that combines the LMS, RLS, and CMA algorithms is proposed to increase the monitoring accuracy of bridge deformation and reduce the measurement error.
- (2) After utilising the improved RLS-CMA for processing various types of modulation signals, it is found that at high SNR values, the correction speed, and anti-intercode interference capability of this algorithm exceed those of the CMA. The lower the error vector amplitude, the higher the accuracy of the

received constellation. The EVM of the improved RLS-CMA equalisation algorithm is smaller than those of the CMA equalisation and nonequalisation algorithms, while its accuracy is increased by 17%.

- (3) According to the results of the engineering case study, the error vector amplitude accuracy of the 16PSK modulation signal is 0.206 m at SNR = 0 dB, 0.037 m at SNR = 4 dB, 0.047 m at SNR = 8 dB, 0.083 m at SNR = 12 dB, 0.150 m at SNR = 16 dB, 0.199 m at SNR = 20 dB, and 0.217 m at SNR = 24 dB. These parameters satisfy the deformation monitoring requirements established for long-span bridges.

Although the RLS-CMA considerably reduces the intercode interference into the transmitted Beidou monitoring signal, the following steps are required for its practical implementation:

- (1) Despite the satisfactory results achieved by the RLS-CMA, the latter has not completely eliminated the intercode interference generated during the signal transmission of the Beidou satellite but significantly decreased it compared with the effects produced by the previously developed algorithms. Therefore, the algorithm proposed in this study should be further improved, or another algorithm should be created for complete ISI elimination.
- (2) In this study, only the ISI into the transmission signals of the Beidou monitoring system is considered. However, many other factors affect the monitoring accuracy of the Beidou system, such as the corrections of the satellite clock error and ionospheric delay.
- (3) Bridge deformation is a complex process. This work does not analyse the relationship between the measurement results and the bridge structure.

Data Availability

The data used to support the findings of this study are included in the article.

Conflicts of Interest

The authors declare that there are no conflicts of interest regarding the publication of this paper.

Acknowledgments

The authors would like to acknowledge the financial support provided through the National Key R&D Program of China (grant nos. 2018YFC0809600 and 2018YFC0809606).

References

- [1] N. Panizel and M. Pinchas, "An approximated expression for the residual ISI obtained by blind adaptive equalizer and biased input signals," *Journal of Signal and Information Processing*, vol. 5, no. 4, pp. 155–178, 2014.
- [2] M. Pinchas, "Convergence curve for non-blind adaptive equalizers," *Journal of Signal and Information Processing*, vol. 07, no. 01, pp. 7–17, 2016.
- [3] M. Pinchas, "Two blind adaptive equalizers connected in series for equalization performance improvement," *Journal of Signal and Information Processing*, vol. 04, no. 01, pp. 64–71, 2013.
- [4] C. Chih-Chun Feng and C. Chong-Yung Chi, "Performance of cumulant based inverse filters for blind deconvolution," *IEEE Transactions on Signal Processing*, vol. 47, no. 7, pp. 1922–1935, 1999.
- [5] M. A. Demir and A. Ozen, "A novel variable step size adjustment method based on autocorrelation of error signal for the constant modulus blind equalization algorithm," *Radio-engineering*, vol. 21, pp. 37–45, 2012.
- [6] R. Hamzehyan, R. Dianat, and N. C. Shirazi, "New variable step-size blind equalization based on modified constant modulus algorithm," *International Journal of Machine Learning and Computing*, vol. 2, pp. 30–34, 2012.
- [7] X. Zhang, L. S. Li, D. F. Zhuo, Z. S. Dong, and L. Zhang, "A new adaptive step-size blind equalization based on autocorrelation of error signal," in *Proceedings of the 7th international conference on signal processing*, pp. 1719–1722, Beijing, September 2004.
- [8] O. Shalvi and E. Weinstein, "New criteria for blind deconvolution of nonminimum phase systems (channels)," *IEEE Transactions on Information Theory*, vol. 36, no. 2, pp. 312–321, 1990.
- [9] Y. Xiao, "Underwater acoustic channel constant modulus algorithm blind equalization: theory," *Algorithm and Simulation*, Posts & Telecom Press, Beijing, 2015.
- [10] B. Baykal and A. G. Constantinides, "Matched filtering for CMA-based blind channel estimation," *Electronics Letters*, vol. 39, no. 17, pp. 1285–1287, 2003.
- [11] S. A. Athuraliya and L. M. Garth, "Quantized CMA equalization for shaped signal constellations," *IEEE Signal Processing Letters*, vol. 11, no. 2, pp. 67–70, 2004.
- [12] Y. Xiao, Y. Dong, and J. Sun, "An adaptive momentum CMA blind equalization based on error energy," *International Journal of Communications, Network and System Sciences*, vol. 10, no. 05, pp. 333–340, 2017.
- [13] L. Y. Zhang, L. Chen, and Y. S. Sun, "Variable step-size CMA blind equalization based on non-linear function of error signal," *Proceedings of the International Conference on Communications and Mobile Computing*, vol. 2009, pp. 396–399, 2009.
- [14] M. Amin, H. Lin, C. R. Reed, and R. Malkemes, "A modified constant modulus algorithm for adaptive channel equalization for QAM signals," in *Proceedings of the 11th IEEE signal processing workshop*, pp. 563–566, Singapore, August 2001.
- [15] X. Dai, "CMA-based nonlinear blind equaliser modelled by a two-layer feedforward neural network," *IEE Proceedings - Communications*, vol. 148, no. 4, pp. 243–248, 2001.
- [16] Y. Ni, X. Du, R. Xiao, and R. Xie, "Multi-modulus blind equalization algorithm based on high-order QAM genetic optimization," in *Proceedings of the 2012 8th International Conference on Natural Computation*, pp. 679–682, Chongqing, China, May 2012.
- [17] D. Wang and S. Chandana, "Nonlinear blind equalizers: NCMA and NMCMA," *International Journal of Communications, Network and System Sciences*, vol. 03, no. 06, pp. 523–529, 2010.
- [18] J. Yu and N. Chi, *Digital Signal Processing in High-Speed Optical Fiber Communication Principle and Application*, Springer Nature, Singapore, 2020.
- [19] W. Han and P. Que, "A modified wavelet transform domain adaptive FIR filtering algorithm for removing the SPN in the MFL data," *Measurement*, vol. 39, no. 7, pp. 621–627, 2006.
- [20] G. Kaur and G. Kaur, "Simulation and comparative analysis of SS-LMS & RLS algorithms for electronic dispersion compensation," *Open Access Library Journal*, vol. 1, p. e676, 2014.
- [21] F. Xu, L. D. Qiu, and Y. Wang, "Hybrid blind equalizing method for APSK signals," *Journal of Chongqing University of Posts and Telecommunications (Natural Science Edition)*, vol. 25, pp. 605–610, 2013.
- [22] Z.-l. Wang, X.-w. Zhang, J.-b. Yang, and G. Chen, "Study of a new fast adaptive filtering algorithm," *Frontiers of Electrical and Electronic Engineering in China*, vol. 1, no. 3, pp. 334–339, 2006.
- [23] S. A. Tretter, *Communication system design using DSP algorithms with laboratory experiments for the TMS320C6713™ DSK*, Springer Science & Business Media LLC, NJ, USA, 2008.
- [24] M. Pinchas, "A MSE optimized polynomial equalizer for 16QAM and 64QAM constellation," *Signal, Image and Video Processing*, vol. 5, no. 1, pp. 29–37, 2011.
- [25] Y. Su, X. Lu, L. Huang, X. Du, and M. Guizani, "A novel DCT-based compression scheme for 5G vehicular networks," *IEEE Transactions on Vehicular Technology*, vol. 68, Article ID 10872, 2019.
- [26] L. Bao, C. Zhao, X. Xue, and L. Yu, "Improved dark channel defogging algorithm for defect detection in underwater structures," *Advances in Materials Science and Engineering*, vol. 2020, Article ID 8760324, 13 pages, 2020.